Policy Research Journal
ISSN (E): 3006-7030 ISSN (P) : 3006-7022 Volume 4, Issue 4, 2026

EXACT SOLUTION OF PLANE WAVE DIFFRACTION IN SEMI INFINITE PARALLEL PLATE WAVEGUIDES USING THE MATRIX WIENER-HOPF EQUATION

Ghulam Yameen Mallah[*1], Mehboob Ali Jatoi[2], Izhar Ali Amur[3], Munwar Ayaz Memon[4], Muzaffar Bashir Arain[5]

[*1]*Department of Basic Science and Related Studies,Quaid-e-Awam University of Engineering, Science and Technology, 67480 Nawabshah, Sindh, Pakistan*
[2]*Department of Basic Science and Related Studies,Quaid-e-Awam University of Engineering, Science and Technology, 67480 Nawabshah, Sindh, Pakistan*
[3]*Department of Basic Science and Related Studies, Shaheed Benazir Bhutto University, Shaheed Benazirabad, 67480, Pakistan*
[4]*Department of Electrical Engineering, Quaid-e-Awam University of Engineering, Science and Technology, 67480 Nawabshah, Sindh, Pakistan*
[5]*Department of Mathematics and Statistics,Quaid-e-Awam University of Engineering, Science and Technology, 67480 Nawabshah, Sindh, Pakistan*

[*1]gh.yameen@quest.edu.pk

DOI: https://doi.org/10.5281/zenodo.19879148

Keywords
Wiener-Hopf technique, plane wave diffraction, parallel-plate waveguide, Fourier transform, electromagnetic scattering, semi-infinite waveguide.

Article History

Received on 30 March, 2025
Accepted on 27 April, 2026
Published on 29 April, 2026

Corresponding Author: * Ghulam Yameen Mallah

Abstract

This paper investigates the diffraction of a time-harmonic plane electromagnetic wave by a parallel-plate waveguide with mixed boundary conditions, consisting of a Neumann upper plate and a Dirichlet lower plate. The waveguide geometry comprises a two-part impedance plane combined with a perfectly conducting plate, forming a semi-infinite structure. By applying Fourier transform techniques, the Helmholtz equation governing the wave field is reduced to a matrix Wiener–Hopf equation, which is solved using kernel factorization and analytic continuation. The solution leads to two coupled infinite systems of linear algebraic equations corresponding to the unknown spectral functions. The effects of waveguide height, incidence angle, and mixed boundary conditions on the diffracted field are analyzed. The results indicate that the Neumann–Dirichlet combination significantly modifies the field distribution compared to symmetric boundary cases, particularly in the far-field scattering pattern. The proposed methodology provides a coherent framework for investigating diffraction in waveguides with mixed boundaries and is applicable to electromagnetic shielding, waveguide irregularities, and acoustic systems. It also incorporates recent advances in Wiener-Hopf techniques, emphasizing the relevance and novelty of this extended formulation.

1. Introduction

Wave propagation and diffraction in guided structures remain central topics in applied mathematics, mathematical physics, and electromagnetic theory. Parallel-plate waveguides have been extensively studied because they combine analytical simplicity with practical importance in microwave engineering, optical systems, shielding enclosures, and scattering from open-ended cavities. Typically, these problems are modelled using the Helmholtz equation together with boundary conditions that reflect the physical surfaces of the waveguide. However, when the geometry includes discontinuities such as open ends, junctions or mixed-material surfaces so that the boundary-value problem becomes more complex and often requires advanced analytical methods [1], [2]. One of the most powerful techniques for such problems is the Wiener–Hopf method, which can produce exact or formally exact solutions for semi-infinite or piecewise-uniform structures. Classical applications include diffraction by half-planes, wedges, impedance plates, and open-ended waveguides [3], [4], [5]. Modern systems, however, often involve hybrid materials, asymmetrical boundaries, and irregular waveguide shapes, introducing new analytical challenges [6], [7].

Recent research has extended Wiener–Hopf methods to more complex problems. Generalized Wiener–Hopf equations have been developed to handle angular or flanged geometries with inhomogeneous media [8], [9]. Iterative and approximate methods for matrix Wiener–Hopf problems now allow factorization of coupled kernels that previously required fully analytical decomposition [10]. Fast numerical techniques using Fourier and Hilbert transforms also enable the solution of both scalar and matrix Wiener–Hopf equations efficiently [11]. For parallel-plate waveguides, significant advances include exact Wiener–Hopf solutions for multi-layer dielectric loading, covering both E- and H-polarizations [12], [13]. Partial material loading has been addressed by combining Wiener–Hopf with modified residue calculus techniques (MRCT), producing accurate field reconstruction [14], [15]. The diffraction of plane waves by semi-infinite waveguides with perfect-conductor loading has also been solved using Fourier transform and Wiener–Hopf, yielding closed-form expressions for the scattered field [16]. Theoretical contributions have clarified scattering from semi-infinite plates with two-sided linear boundary conditions, allowing analysis of asymmetrical surfaces [17]. Further studies focus on factorization of matrix Wiener–Hopf kernels in acoustic or electromagnetic contexts, including waveguide barriers, collinear cracks, and plate arrays [18], [19]. Wiener–Hopf has also been applied to novel configurations such as semi-infinite circular pins, showing its flexibility in structural-acoustic problems [20], [21].

Recent contributions include exact solutions for semi-infinite guides with five-layer material loading [12], partial loading with modified residue calculus techniques (MRCT) [14], and plane-wave diffraction by perfectly conducting rectangular cylinders [15], [16], [22]. Waveguide-like scattering problems with cylindrical or corrugated geometries have been solved using Wiener–Hopf–Fock formulations [23]. Beyond electromagnetics, Wiener–Hopf is now relevant in plasmonic, nano-photonics, and electrostatics. For example, edge diffraction in plasmon launching and the electrostatic field around circular cylinders with slots have been analysed using Wiener–Hopf, demonstrating its versatility in both electromagnetic and structural-acoustic contexts [24], [25].

Despite these advances, a significant gap persists in fully asymmetric parallel-plate waveguides, where the two bounding surfaces have different material or impedance properties, have rarely been analysed using exact analytical methods. Most studies assume symmetry or rely heavily on numerical approximation for asymmetrical cases [12], [14], [16], [22]. This gap limits theoretical understanding and the design of asymmetric open-ended structures used in sensing, shielding, and waveguide-based devices.

In this paper, we address this gap by studying a time-harmonic plane wave incident on a semi-infinite parallel-plate waveguide with different boundary conditions on each plate. Applying the Fourier transform to the Helmholtz equation, we derive a matrix Wiener–Hopf equation, which is

factorized using analytic continuation and canonical decomposition. This results in two infinite systems of linear algebraic equations for the spectral amplitudes, allowing exact reconstruction of the scattered field. The results provide insights into the effects of waveguide height, incident angle, and boundary asymmetry on diffraction, serving as analytical benchmarks for practical applications.

The paper is organized as follows: Section 2 presents the mathematical modelling of the governing equations for the forced nonlinear transverse vibrations of a moving beam with an elastic foundation and damping. Section 3 outlines the development of asymptotic expansion using the two-timescale method to assess system stability. Section 4 discusses the dynamic stability characteristics within resonance regions. Finally, section 5 provides the conclusions derived from the study.

2. Mathematical Formulation and Geometry

The diffraction of a time-harmonic plane electromagnetic wave is considered by a semi-infinite parallel-plate waveguide occupying the region $0 < y < b,\ x > 0$, where $b > 0$ denotes the plate separation. The wave guide open at $x = 0$ and extends infinitely in the z-direction, allowing the field to be treated as a two-dimensional problem. The plates are assumed to be perfectly conducting, except for the distinction in their surface behavior, which is encoded in the boundary conditions imposed on the scalar field.

For a transverse incident wave, the E_z-polarized plane wave filed must satisfy the Helmholtz equation and given by

$$\frac{\partial^2 u}{\partial x^2} + \frac{\partial^2 u}{\partial y^2} + k^2 u = 0, \tag{1}$$

where k is a wave number. The structure consists of two parallel plates located at $y = 0$ and $y = b$, which form semi-infinite waveguide in the region $x > 0$. The half plane $0 < y < b,\ x < 0$ is unbounded and represents the exterior region into which wave is incident. The lower plate is held at a fixed potential, while the upper plate enforces a vanishing normal derivative of the field. Mathematically, these Dirichlet condition at the lower plate and Neuman condition at the upper plate are expressed respectively as:

$$u(x, 0) = 0, \quad x > 0, \tag{2}$$

and

$$\frac{\partial}{\partial y} u(x, b) = 0, \quad x > 0. \tag{3}$$

3. Formulation of Matrix Wiener-Hopf Equation

Consider the diffraction in a time harmonic E_z-polarized plane wave,

$$u_i(x, y) = e^{-ik(x\cos\theta_0 - y\sin\theta_0)}, \tag{4}$$

The parallel-plate waveguide formed by a two-part impedance plane placed at y = 0 and a parallel perfectly conducting half-plane placed at $\{x < 0, y = 0,\ z \in (-\infty, \infty)\}$ is also considered. We shall assume that k has a small imaginary part for the sake of analytical convenience and the surrounding medium is somewhat lossy, so at the end of analysis it can be obtained by making $\mathrm{Im}(k) \to 0$. The surface impedance of the parts $x < 0$ and $x > 0$ of the plane $y = 0$, relative to the characteristic impedance of free space, are assumed to be η_1 and η_2, respectively.

The total field can be expressed as

$$u^T(x, y) = \begin{cases} u_i(x, y) + u_r(x, y) + u_1(x, y), & y > b \\ u_2(x, y), & 0 < y < b \end{cases}, \tag{5}$$

where u_i is the incident field given by Eq. (4) and if the whole plane is perfectly conducting then u_r will be the reflected field

$$u_r(x, y) = -e^{-ik(x\cos\theta_0 - (y-2b)\sin\theta_0)}. \tag{6}$$

The unknown fields u_1 and u_2, which satisfy the Helmholtz equation

$$\left(\frac{\partial^2}{\partial x^2} + \frac{\partial^2}{\partial y^2} + k^2\right) u_j(x, y) = 0, \quad j = 1,2. \tag{7}$$

It is convenient to use the following representations of Fourier integral as

$$u_1(x,y) = \frac{1}{2\pi}\int_L A_1(\alpha)e^{iK(y-b)-i\alpha x}d\alpha, \quad (8)$$

and

$$u_2(x,y) = \frac{1}{2\pi}\int_L [B_1(\alpha)\cos ky + C_1(\alpha)\alpha \sin Ky]e^{-i\alpha x}d\alpha, \quad (9)$$

with

$$K(\alpha) = \sqrt{k^2-\alpha^2}. \quad (10)$$

The function in Eq. (10) is defined in the complex α-plane with cut along $\alpha = k$ to $\alpha = k + i\infty$ and $\alpha = -k$ to $\alpha = -k - i\infty$, such that $K(\alpha) = k$. By considering the asymptotic behaviours of u_1 and u_2, for $|x| \to \infty$ as

$$v_1(x,y) = \begin{cases} O\left(e^{-ikx\cos\theta_0}\right), & x \to \infty \\ O\left(e^{-ikx}/\sqrt{-x}\right), & x \to -\infty \end{cases}, \quad (11)$$

$$v_2(x,y) = O\left(e^{-ik|x|}/\sqrt{|x|}\right), \quad |x| \to \infty. \quad (12)$$

The integration line L is a straight line parallel to the real α-axis lying in the strip $\mathrm{Im}(k\cos\theta_0) < \mathrm{Im}(\alpha) < \mathrm{Im}(k)$. The unknown coefficients $A_1(\alpha)$, $B_1(\alpha)$ and $C_1(\alpha)$, which are to be determined with the aid of the following boundary and continuity relations.

$$\frac{\partial}{\partial y}u_1(x,b) = 0, \quad x < 0, \quad (13)$$

$$u_1(x,b) - u_2(x,b) = 0, \quad x \in (-\infty,\infty), \quad (14)$$

$$\frac{\partial}{\partial y}u_1(x,b) + \frac{\partial}{\partial y}u_i(x,b) + \frac{\partial}{\partial y}u_r(x,b) - \frac{\partial}{\partial y}u_2(x,b) = 0, \quad x > 0, \quad (15)$$

$$\left(1 + \frac{\eta_1}{ik}\frac{\partial}{\partial y}\right)u_2(x,0) = 0, \quad x < 0, \quad (16)$$

$$\left(1 + \frac{\eta_2}{ik}\frac{\partial}{\partial y}\right)u_2(x,0) = 0, \quad x > 0. \quad (17)$$

The uniqueness of the mixed boundary value problem defined by the Helmholtz equation required the satisfaction of radiation condition,

$$\sqrt{\rho}\left[\frac{\partial u}{\partial \rho} - iku\right] \to 0, \quad \rho = \sqrt{x^2+y^2} \to \infty, \quad (18)$$

and the edge conditions near origin $(0,0)$ and the point $(0,b)$

$$u^T(x,y) = O\left(|x|^{\frac{1}{2}}\right), \quad |x| \to 0, \quad (19)$$

$$\frac{\partial}{\partial y}u^T(x,y) = O\left(|x|^{-\frac{1}{2}}\right), \quad |x| \to 0. \quad (20)$$

By substituting Eq. (8) into Eq. (13), the expression takes the following form:

$$\frac{\partial}{\partial y}u_1(x,b) == \frac{iK}{2\pi}\int_{-\infty}^{0} A_1(\alpha)e^{-i\alpha x}d\alpha, \quad (21)$$

By inverting the above integral equation, the resulting expression becomes:

$$\int_0^\infty u_1(x,b)e^{i\alpha x}dx = iKA_1(\alpha), \quad (22)$$

or it can be written as:

$$A_1(\alpha) = \frac{\psi_1^+(\alpha)}{iK}, \quad (23)$$

where,

$$\psi_1^+(\alpha) = \int_0^\infty u_1(x,b)e^{i\alpha x}dx, \quad (24)$$

and in a same way, Eq. (14) yields:

$$A_1(\alpha) = B_1(\alpha)\cos Kb + C_1(\alpha)\sin Kb, \quad (25)$$

likewise, Eq. (15) provides:

$$iKA_1(\alpha) + K[B_1(\alpha)\sin Kb - C_1(\alpha)\cos Kb] = -\frac{2ke^{-ikb\sin\theta_0}\sin\theta_0}{\alpha - k\cos\theta_0} + \psi_1^-(\alpha), \quad (26)$$

where,

$$\psi_1^-(\alpha) = \int_{-\infty}^{0} \left[\frac{\partial}{\partial y}u_1(x,b) - \frac{\partial}{\partial y}u_2(x,b)\right] e^{i\alpha x}dx, \quad (27)$$

respectively, Eq. (16) and Eq, (17) yield:

$$B_1(\alpha) + \frac{\eta_1}{ik}KC_1(\alpha) = \psi_2^+(\alpha), \quad (28)$$

and

$$B_1(\alpha) + \frac{\eta_2}{ik}KC_1(\alpha) = \psi_2^-(\alpha), \quad (29)$$

with

$$\psi_2^+(\alpha) = \int_0^{\infty}\left(1 + \frac{\eta_1}{ik}\frac{\partial}{\partial y}\right)u_2(x,0)e^{i\alpha x}dx, \quad (30)$$

and

$$\psi_2^-(\alpha) = \int_0^{\infty}\left(1 + \frac{\eta_2}{ik}\frac{\partial}{\partial y}\right)u_2(x,0)e^{i\alpha x}dx. \quad (31)$$

Taking into account the analytic properties of the Fourier integrals, together with Eq. (11) and Eq. (12), where $\psi_{1,2}^+(\alpha)$ and $\psi_{1,2}^-(\alpha)$ remain regular in the half-planes $\mathrm{Im}(\alpha) > \mathrm{Im}(k\cos\theta_0)$ and $\mathrm{Im}(\alpha) < \mathrm{Im}(k)$, respectively.

To determine $B_1(\alpha)$ and $C_1(\alpha)$, Eq. (22) and Eq. (23) are employed, resulting in:

$$B_1(\alpha) = \frac{\eta_2\psi_2^+(\alpha) - \eta_1\psi_2^-(\alpha)}{\eta_2 - \eta_1}, \quad (32)$$

$$C_1(\alpha) = \frac{ik\{\psi_2^-(\alpha) - \psi_2^+(\alpha)\}}{K(\eta_2 - \eta_1)}. \quad (33)$$

By substituting Eq. (23), Eq. (32) and Eq. (33) into Eq. (25) and Eq. (26), a pair of coupled Wiener-Hopf equations is obtained, given respectively as:

$$\psi_1^+(\alpha) - \frac{\psi_2^+(\alpha)}{\eta_2 - \eta_1}\left(\eta_2\cos Kb - ik\frac{\sin Kb}{K}\right) + \frac{\psi_2^-(\alpha)}{\eta_2 - \eta_1}\left(\eta_1\cos Kb - ik\frac{\sin Kb}{K}\right) = 0, \quad (34)$$

$$\psi_1^+(\alpha) + \frac{\psi_2^+(\alpha)}{\eta_2 - \eta_1}(\eta_2 K\sin Kb + ik\cos Kb) - \frac{\psi_2^-(\alpha)}{\eta_2 - \eta_1}(\eta_1 K\sin Kb + ik\cos Kb) = \psi_1^-(\alpha) - \frac{2k\sin\theta_0}{\alpha - k\cos\theta_0}e^{-ikb\sin\theta_0}. \quad (35)$$

In matrix form, the system becomes:

$$\begin{bmatrix} 1 & -i\eta_2\cos Kb - k\sin Kb \\ 1 & \eta_2 K\sin Kb + ik\cos Kb \end{bmatrix}\begin{bmatrix} \psi_1^+(\alpha) \\ \frac{\psi_2^+(\alpha)}{\eta_2 - \eta_1} \end{bmatrix} + \begin{bmatrix} 0 & i\eta_1\cos Kb + k\sin Kb \\ -1 & \eta_1 K\sin Kb + ik\cos Kb \end{bmatrix}\begin{bmatrix} \psi_1^-(\alpha) \\ \frac{\psi_2^-(\alpha)}{\eta_2 - \eta_1} \end{bmatrix} = \begin{bmatrix} 0 \\ -\frac{2k\sin\theta_0}{\alpha - k\cos\theta_0}e^{-ikb\sin\theta_0} \end{bmatrix}. \quad (36)$$

3.1 Solution of the Simultaneous Wiener-Hopf Equations

For solving the simultaneous Wiener-Hopf equations given in Eq. (34) and Eq. (35), it is convenient first to rewrite Eq. (34) as:

$$\frac{(\eta_2 - \eta_1)\psi_1^+(\alpha)}{\mathrm{ikKM_1}(\eta_2,\alpha)} + \psi_2^+(\alpha) = \psi_2^-(\alpha)\mathrm{L}(\alpha), \quad (37)$$

where,

$$\mathrm{L}(\alpha) = \frac{\mathrm{M_1}(\eta_1,\alpha)}{\mathrm{M_1}(\eta_2,\alpha)}, \quad (38)$$

and

$$\mathrm{M_1}(\eta_j,\alpha) = \mathrm{i}\frac{\sin \mathrm{Kb}}{\mathrm{K}} - \frac{\eta_j}{\mathrm{k}}\cos \mathrm{Kb}, \quad j = 1,2. \quad (39)$$

By multiplying Eq. (34) by $(\eta_2 K\sin Kb + ik\cos Kb)$ and Eq. (35) by $(\eta_2 iK\cos Kb + k\sin Kb)$, and subsequently adding the resulting equations, the following equation is obtained:

$$\frac{\psi_1^+(\alpha)}{\mathrm{N}(\alpha)} - \frac{\psi_2^-(\alpha)}{\mathrm{M_2}(\eta_2,\alpha)} = -\psi_1^-(\alpha) + \frac{2k\sin\theta_0}{\alpha - k\cos\theta_0}e^{-ikb\sin\theta_0}, \quad (40)$$

where,

$$M_2(\eta_2,\alpha)=\frac{\sin Kb}{K}+\frac{i\eta_2}{k}\cos Kb, \quad (41)$$

$$N(\alpha)=M_3(\eta_2,\alpha)R(\eta_2,\alpha)e^{iKb}, \quad (42)$$

$$M_3(\eta_2,\alpha)=\frac{ik\sin Kb}{K}+\eta_2\cos Kb, \quad (43)$$

$$R(\eta_2,\alpha)=\left(\eta_2+\frac{k}{K(\alpha)}\right)^{-1}. \quad (44)$$

Rewriting the Wiener–Hopf equation in Eq. (37) yields the following form:

$$\frac{\psi_1^+(\alpha)}{K(\alpha)M_1(\eta_2,\alpha)L^+(\alpha)}+\frac{ik\psi_2^+(\alpha)}{(\eta_2-\eta_1)L^+(\alpha)}+\psi_2^+(\alpha)=\frac{ik}{\eta_2-\eta_1}\psi_2^-(\alpha)L^-(\alpha), \quad (45)$$

where, $L^+(\alpha)$ and $L^-(\alpha)$ denote the regular functions that are free of zeros in the upper and lower half-planes, respectively. Using the Wiener-Hopf factorization of the meromorphic function $L(\alpha)$, one obtains:

$$L(\alpha)=L^+(\alpha)L^-(\alpha), \quad (46)$$

Explicit expressions can easily be obtained as follows:

$$L^+(\alpha)=\left(\frac{i\sin kb-\eta_1\cos kb}{k}\right)^{\frac{1}{2}}\left(\frac{i\sin kb-\eta_2\cos kb}{k}\right)^{-\frac{1}{2}}\prod_{n=0}^{\infty}\left(1+\frac{\alpha}{\alpha_n}\right)\left(1+\frac{\alpha}{\beta_n}\right)^{-1}, \quad (47)$$

where, $\alpha=\pm\alpha_n$ are the zeros of the function $M_1(\eta_1,\alpha)$ and $\alpha=\pm\beta_n$ are the zeros of $M_1(\eta_2,\alpha)$. In the upper half-plane, the left-hand side of Eq. (45) is regular except at the poles of the first term, which correspond to the zeros of $M_1(\eta_2,\alpha)$located there, specifically at $\alpha=\beta_n$, with,

$$M_1(\eta_2,\pm\beta_n)=0, \quad Im(\beta_n)>Im(k) \quad (48)$$

Subtracting the infinite set of poles from both sides of Eq. (45) results in:

$$\frac{\psi_1^+(\alpha)}{K(\alpha)M_1(\eta_2,\alpha)L^+(\alpha)}-\sum_{n=0}^{\infty}\frac{p_n}{\alpha-\beta_n}+\frac{ik\psi_2^+(\alpha)}{(\eta_2-\eta_1)L^+(\alpha)}+\psi_2^+(\alpha)=\frac{ik}{\eta_2-\eta_1}\psi_2^-(\alpha)L^-(\alpha)--\sum_{n=0}^{\infty}\frac{p_n}{\alpha-\beta_n}, \quad (49)$$

where,

$$p_n=\frac{\psi_1^+(\beta_n)}{K(\beta_n)\dot{M}_1(\eta_2,\beta_n)L^+(\beta_n)}, \quad n=1,2,3\ldots, \quad (50)$$

$\dot{M}_1(\eta_2,\beta_n)$ denotes the differentiation with respect to α. Applying the principle of analytical continuation and Liouville's theorem to Eq. (49) gives:

$$\psi_2^-(\alpha)L^-(\alpha)=\frac{ik}{\eta_2-\eta_1}\sum_{n=0}^{\infty}\frac{p_n}{\alpha-\beta_n}, \quad (51)$$

$$\frac{\psi_2^+(\alpha)}{L^+(\alpha)}=\frac{\eta_2-\eta_1}{ik}\sum_{n=0}^{\infty}\frac{p_n}{\alpha-\beta_n}-\frac{(\eta_2-\eta_1)\psi_1^+(\alpha)}{ikK(\alpha)M_1(\eta_2,\alpha)L^+(\alpha)}. \quad (52)$$

The scalar kernel $N(\alpha)$ in the Wiener-Hopf equation of Eq. (40) can be expressed as a product of two functions, $N^+(\alpha)$ and $N^-(\alpha)$, where $N^+(\alpha)$ is regular and free of zeros in the region $Im\ \alpha > Im\ (k\cos\theta_0)$, and $N^-(\alpha)$ is regular and free of zeros in the region $Im\ \alpha < Im\ k$.

The kernel functions in Eq. (40), namely $N(\alpha)$ and $R(\eta_j,\alpha)$, can be factorized using established expressions. Consequently, the factors of $N(\alpha)$ are:

$$N^+(\alpha)=R^+(\eta_2,\alpha)(i\sin kb-\eta_2\cos kb)^{\frac{1}{2}}e^{\left\{\frac{Kb}{\pi}\ln\left(\frac{\alpha+iK}{k}\right)\right\}+\left\{\frac{i\alpha b}{\pi}\left(1-c+\ln\left(\frac{2\pi}{kb}\right)+\frac{i\pi}{2}\right)\right\}}\prod_{n=1}^{\infty}\left(1+\frac{\alpha}{\beta_n}\right)e^{\frac{i\alpha b}{n\pi}}, \quad (53)$$

and

$$N^-(\alpha)=N^+(-\alpha), \quad (54)$$

In Eq. (53), c denotes the Euler constant, whose value is approximately $0.577215\ldots$. The factors of $R(\eta_j,\alpha)$ can be expressed in terms of the Malyuzhinetz functions as:

$$R^-(\eta_j,k\cos\theta)=\frac{4}{\sqrt{\eta_j}}\sin\left(\frac{\emptyset}{2}\right)\left\{\frac{M_\pi\left(\frac{3\pi}{2}-\theta-\emptyset\right)M_\pi\left(\frac{\pi}{2}-\theta+\emptyset\right)}{M_\pi^2\left(\frac{\pi}{2}\right)}\right\}^2\left\{1+\sqrt{2}\cos\left(\frac{\frac{3\pi}{2}-\theta-\emptyset}{2}\right)\right\}\left\{1+\sqrt{2}\cos\left(\frac{\frac{\pi}{2}+\theta-\emptyset}{2}\right)\right\}^{-1}, \quad (55)$$

and

$$R^{+}(\eta_j, k\cos\theta) = R^{-}(\eta_j, -k\cos\theta), \quad (56)$$

where $M_\pi(z)$ and $\emptyset$ are defined as:

$$M_\pi(z) = e^{-\frac{1}{8\pi}\int_0^z \left(\frac{\pi\sin(u) - 2\sqrt{2}\pi\sin\left(\frac{u}{2}\right) + 2u}{\cos(u)}\right)du}, \quad (57)$$

and

$$\sin(\emptyset) = \frac{1}{\eta_j}, \quad (58)$$

Equation (40) can now be rewritten as:

$$\psi_1^{-}(\alpha)N^{-}(\alpha) - \frac{N^{-}(\alpha)\psi_2^{-}(\alpha)}{M_2(\eta_2,\alpha)} = -\frac{\psi_1^{+}(\alpha)}{N^{+}(\alpha)} + \frac{2k\sin\theta_0}{\alpha - k\cos\theta_0}e^{-ikb\sin\theta_0}N^{-}(\alpha), \quad (59)$$

By applying the additive decomposition to the last term on the right-hand side of Eq. (59), one obtains:

$$\frac{2k\sin\theta_0}{\alpha - k\cos\theta_0}e^{-ikb\sin\theta_0}N^{-}(\alpha) = \frac{2k\sin\theta_0}{\alpha - k\cos\theta_0}e^{-ikb\sin\theta_0}\{N^{-}(\alpha) - N^{-}(k\cos\theta_0)\} + \frac{2k\sin\theta_0}{\alpha - k\cos\theta_0}e^{-ikb\sin\theta_0}N^{-}(k\cos\theta_0), \quad (60)$$

substituting this into Eq. (59) yields:

$$\psi_1^{-}(\alpha)N^{-}(\alpha) - \frac{N^{-}(\alpha)\psi_2^{-}(\alpha)}{M_2(\eta_2,\alpha)} - \frac{2k\sin\theta_0}{\alpha - k\cos\theta_0}e^{-ikb\sin\theta_0}\{N^{-}(\alpha) - N^{-}(k\cos\theta_0)\} = -\frac{\psi_1^{+}(\alpha)}{N^{+}(\alpha)} + \frac{2k\sin\theta_0}{\alpha - k\cos\theta_0}e^{-ikb\sin\theta_0}N^{-}(k\cos\theta_0), \quad (61)$$

thus, on the left-hand side, regularity in the lower region is disrupted by the simple poles associated with the zeros of $M_2(\eta_2, \alpha)$ located there, namely at $\alpha = -\beta_n$. Upon subtracting this infinite set of poles from both sides of Eq. (61), the following expression is obtained:

$$\psi_1^{-}(\alpha)N^{-}(\alpha) - \frac{N^{-}(\alpha)\psi_2^{-}(\alpha)}{M_2(\eta_2,\alpha)} - \sum_{n=0}^{\infty}\frac{q_n}{\alpha+\beta_n} - \frac{2k\sin\theta_0}{\alpha - k\cos\theta_0}e^{-ikb\sin\theta_0}\{N^{-}(\alpha) - N^{-}(k\cos\theta_0)\} = -\frac{\psi_1^{+}(\alpha)}{N^{+}(\alpha)} + \frac{2k\sin\theta_0}{\alpha - k\cos\theta_0}e^{-ikb\sin\theta_0}N^{-}(k\cos\theta_0) - \sum_{n=0}^{\infty}\frac{q_n}{\alpha+\beta_n}, \quad (62)$$

where q_m satisfies

$$q_n = \frac{N^{+}(\beta_n)\psi_1^{-}(-\beta_n)}{\dot{M}_2(\eta_2,-\beta_n)}, \quad n = 1,2,3\ldots, \quad (63)$$

Applying the principle of analytical continuation and Liouville's theorem to Eq. (62) gives:

$$\frac{\psi_1^{+}(\alpha)}{N^{+}(\alpha)} = \frac{2k\sin\theta_0}{\alpha - k\cos\theta_0}e^{-ikb\sin\theta_0}N^{-}(k\cos\theta_0) - \sum_{n=0}^{\infty}\frac{q_n}{\alpha+\beta_n}, \quad (64)$$

$$\psi_1^{-}(\alpha)N^{-}(\alpha) = \frac{N^{-}(\alpha)\psi_2^{-}(\alpha)}{M_2(\eta_2,\alpha)} + \sum_{n=0}^{\infty}\frac{q_n}{\alpha+\beta_n} + \frac{2k\sin\theta_0}{\alpha - k\cos\theta_0}e^{-ikb\sin\theta_0}\{N^{-}(\alpha) - N^{-}(k\cos\theta_0)\}. \quad (65)$$

The solution is expressed as an infinite series of constants p_m and q_m corresponding to the simultaneous Wiener–Hopf equations. Substituting Eq. (64) in Eq. (50) and Eq. (51) in Eq. (58), it can be shown that these constants are determined by solving the following two infinite sets of linear algebraic equations numerically:

$$p_n = \frac{N^{+}(\beta_n)}{\dot{M}_1(\eta_2,\beta_n)L^{+}(\beta_n)}\left(\sum_{n=0}^{\infty}\frac{q_n}{\alpha+\beta_n} - \frac{2k\sin\theta_0}{\alpha - k\cos\theta_0}e^{-ikb\sin\theta_0}N^{-}(k\cos\theta_0)\right), \quad n = 1,2,3\ldots, \quad (66)$$

$$q_n = \frac{N^{+}(\beta_n)}{\dot{M}_2(\eta_2,-\beta_n)L^{+}(\beta_n)}\left(\sum_{n=0}^{\infty}\frac{q_n}{\alpha+\beta_n}\right), \quad n = 1,2,3\ldots. \quad (67)$$

4. Field Analysis and Computational Results

The diffracted field $u_1(x, y)$ can now be determined using Eq. (8):

$$u_1(x,y) = \frac{1}{2\pi}\int_L A_1(\alpha)e^{iK(\alpha)(y-b)-i\alpha x}d\alpha. \quad (68)$$

Since $A_1(\alpha) = \frac{\psi_1^{+}(\alpha)}{iK(\alpha)}$ from Eq. (23), the above integral can be written as:

$$u_1(x,y) = \frac{1}{2\pi}\int_L \frac{\psi_1^{+}(\alpha)}{iK(\alpha)}e^{iK(\alpha)(y-b)-i\alpha x}d\alpha, \quad (70)$$

by applying the change of variables $\alpha = -k\cos(t)$, $x = r\cos(\theta)$ and $y = r\sin(\theta)$, the above integral becomes:

$$u_1(r,\theta) = \frac{1}{2\pi}\int_L \psi_1^+(-k\cos t, b)e^{ikb\sin(t)+ikr\cos(t-\theta)}dt, \quad (71)$$

the saddle point occurs at $t = \theta$, and its contribution yields:

$$u_1(r,\theta) = \frac{e^{i\left(-\frac{\pi}{4}+kr\right)}}{\sqrt{2k\pi r}}e^{ikb\sin\theta}\psi_1^+(-k\cos\theta). \quad (72)$$

Finaly by putting Eq. (62) for ψ_1^+, the solution is

$$u_1(r,\theta) = \frac{e^{\frac{-i\pi}{4}}}{\sqrt{2\pi}}\left\{\frac{e^{-ikb(\sin\theta+\sin\theta_0)}2\sin\theta_0}{(\cos\theta+\cos\theta_0)}N^-(k\cos\theta_0)N^-(k\cos\theta) + e^{-ikb\sin\theta}N^-(k\cos\theta)\sum_{n=0}^{\infty}\frac{q_n}{\beta_n - k\cos\theta}\right\}\frac{e^{ikr}}{\sqrt{kr}}. \quad (73)$$

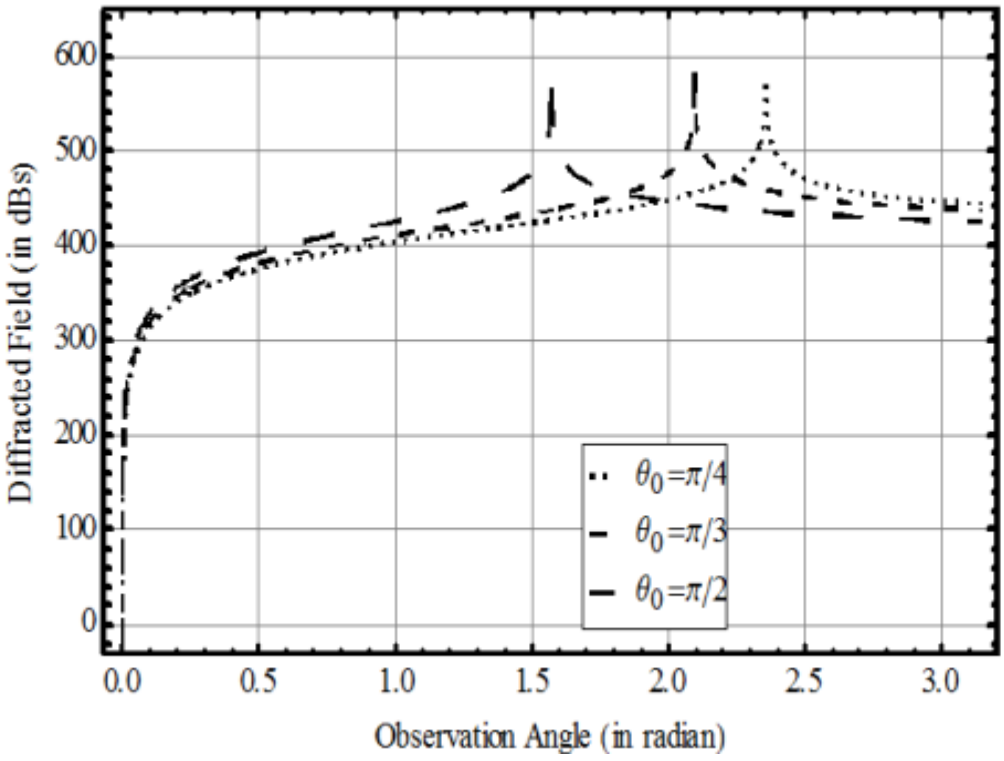

Figure. 1. The variation of diffracted filed with respect to incident angle $\boldsymbol{\theta_0}$ *for* $\boldsymbol{\eta_1 = 0.9i}$, $\boldsymbol{\eta_2 = 0.1i}$ *and* $\boldsymbol{b = 0.2}$.

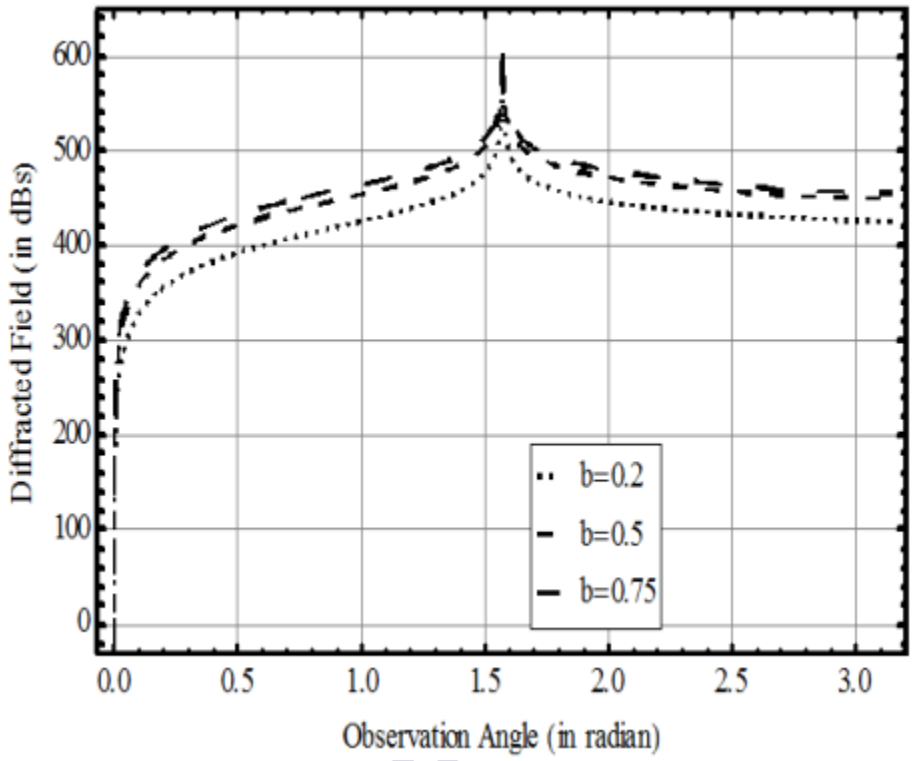

Figure. 2. The variation of diffracted field with respect to separation distance b *for* $\theta_0 = \frac{\pi}{2}$ *for* $\eta_1 = 0.9i$ *and* $\eta_2 = 0.1i$.

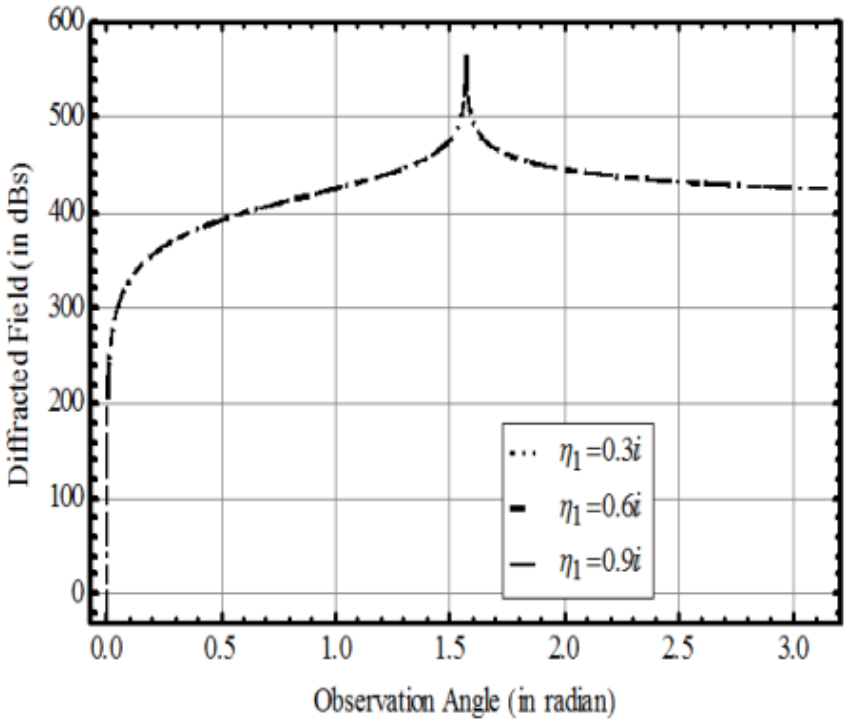

Figure. 3. The variation of diffracted field with respect to $\boldsymbol{\eta_1}$ *for* $\boldsymbol{\theta_0 = \frac{\pi}{2}}$ *for* $\boldsymbol{\eta_2 = 0.1i}$ *and* $\boldsymbol{b = 0.2}$.

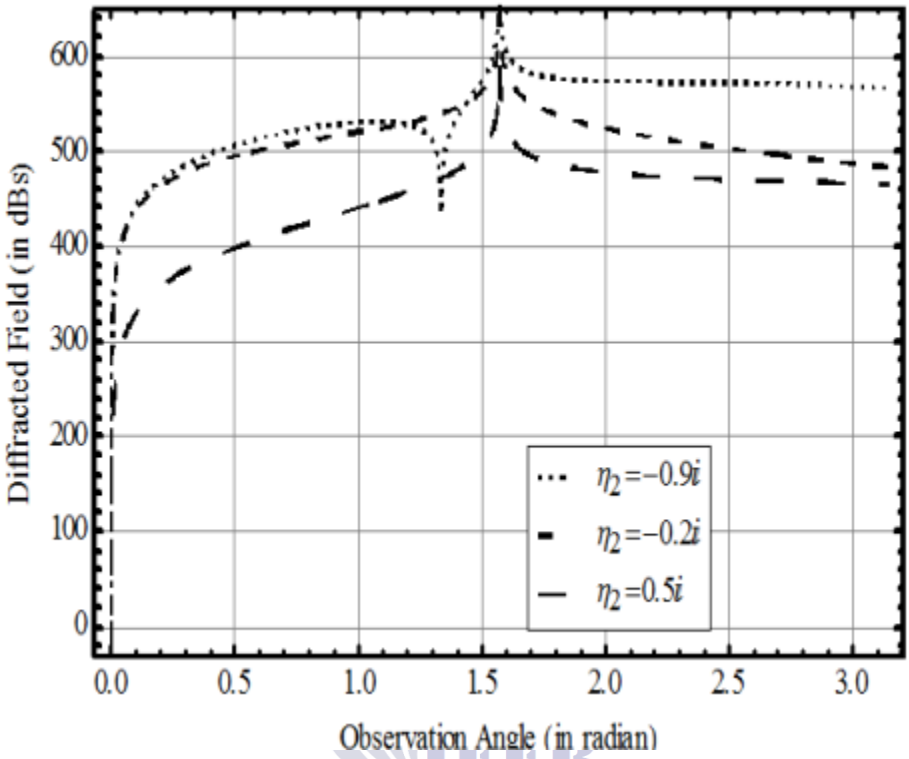

Figure. 4. The variation of diffracted field with respect to $\boldsymbol{\eta_2}$ *for* $\boldsymbol{\theta_0 = \frac{\pi}{2}}$ *for* $\boldsymbol{\eta_1 = 0.1i}$ *and* $\boldsymbol{b = 0.2}$.

As illustrated in Figure. 1, the variation of the diffracted field with observation angle for different θ_0. The field increases, reaches a peak, and then decreases, with θ_0 affecting the peak position and amplitude. The Figure. 2 shows the variation of the diffracted field with observation angle for different b. The field rises to a peak near $\theta \approx 1.5$ radians and then decreases, with larger b giving higher amplitudes. The Figure. 3, the diffraction field exhibits negligible sensitivity to variations in η_1. In addition, Figure. 4 indicate that for $\mathrm{Im}(\eta_2) > 0$, the amplitude of the diffracted field decays rapidly.

5. Conclusion

In this analysis, we have investigated the diffraction of plane wave by parallel plate waveguide with different boundary conditions in a Matrix Wiener-Hopf equation. This problem cannot be directly solved by using the know factorization method, here we have converted the Matrix Wiener-Hopf equation into another form by pre multiplication with a suitable entire matrix. Then the solution of two infinite systems of linear algebraic equations is obtained. These systems are solved numerically under the effect of the parameters such as waveguide spacing and the surface impedance as shown graphically. The main findings of the analysis are:

By decreasing the distance between the two parallel plate, the amplitude of the diffracted field insensitively decreases. By increasing the capacitive surface impedance $\mathrm{Im}(\eta_2) > 0$, the amplitude of the diffracted field decreases.

Data Availability

The data supporting the findings of this study are fully contained within the article.

Conflicts of Interest

The authors declare that there are no conflicts of interest.

REFERENCES

[1] B. Türetken & A. Alkumru, Plane Wave Diffraction by an Open Parallel Plate Waveguide with Dielectric Loading, Math. Comput. Appl., 4(3), 241–249, 1999.

[2] V. G. Daniele & G. Lombardi, Generalized Wiener–Hopf equations for wave motion in angular regions, Proc. R. Soc. A, 477, 20210040, 2021.

[3] V. G. Daniele & G. Lombardi, The generalized Wiener–Hopf equations for the elastic wave motion in angular regions, Proc. R. Soc. A, 478, 20210624, 2022.

[4] A. D. G. Hales & L. J. Ayton, Analytical insights into semi-infinite plate scattering: the Wiener–Hopf technique and two-sided linear boundary conditions, Q. J. Mech. Appl. Math., 77(1-2), 2024.

[5] M. Aitken, On the Factorisation of Matrix Wiener–Hopf Kernels Arising From Acoustic Scattering Problems, PhD Thesis, University of Cambridge, 2024.

[6] N. ul Haq, A. B. Mann & S. Ahmed, Diffraction by Cascaded Thick Half-Planes Composed of PEMC Metamaterial, NUST J. Nat. Sci., 4(1), 8–19, 2018.

[7] K. He & K. Kobayashi, Diffraction by a Semi-Infinite Parallel-Plate Waveguide with Five-Layer Material Loading: H-Polarization, Appl. Sci., 13(6), 3715, 2023.

[8] T. Zhang & K. Kobayashi, Diffraction by a Semi-Infinite Parallel-Plate Waveguide with Partial Material Loading: A Combined Wiener–Hopf & MRCT Solution, IEICE Trans. Electron., E108-C(5), 226–236, 2025.

[9] K. He & K. Kobayashi, Wiener–Hopf Analysis of Plane-Wave Diffraction by a Perfectly Conducting Rectangular Cylinder: H-Polarization, IEICE Trans. Electron., E108-C, 2025.

[10] E. Simakov, S. Galyamin & A. Tyukhtin, Diffraction of a Symmetric TM Mode at an Open-Ended Deeply Corrugated Waveguide with a Small Period, arXiv:2305.04371, 2023.

[11] E. Medvedeva, R. Assier & A. Kisil, Diffraction by a Set of Collinear Cracks on a Square Lattice: An Iterative Wiener–Hopf Method, arXiv:2402.15799, 2024.

[12] K. He & K. Kobayashi, Exact Wiener–Hopf solutions for multi-layer dielectric loading, Appl. Sci., 13, 2023.

[13] K. He & K. Kobayashi, H-Polarization solutions for multi-layer dielectric loading, Appl. Sci., 13, 2023.

[14] J T. Zhang & K. Kobayashi, Partial Material Loading with MRCT and Wiener–Hopf Solution, IEICE Trans. Electron., 108-C, 2025.
[15] K. Kobayashi, Diffraction of Plane Waves by a Semi-Infinite Perfectly Conducting Parallel-Plate Waveguide, Philos. Trans. R. Soc. A, 2025.
[16] K. Kobayashi, Plane-wave diffraction by rectangular cylinders, Philos. Trans. R. Soc. A, 2025.
[17] A. D. G. Hales & L. J. Ayton, Scattering from semi-infinite plates with two-sided boundary conditions, Q. J. Mech. Appl. Math., 77(1-2), 2024.
[18] E. Germano, R. Assier & A. Kisil, Numerical solution of matrix Wiener–Hopf equations using fast Fourier methods, J. Comput. Phys., 2022.
[19] M. Nethercote, A. Kisil & R. Assier, Diffraction of Acoustic Waves by Multiple Semi-Infinite Arrays, arXiv:2306.17657, 2023.
[20] S. Bimurzaev, S. Sautbekov & Z. Sautbekova, Calculation of the Electrostatic Field of a Circular Cylinder with a Slot by Wiener–Hopf, Mathematics, 11(13), 2933, 2023.
[21] S. Bimurzaev, S. Sautbekov & Z. Sautbekova, Circular pin diffraction using Wiener–Hopf, Mathematics, 11, 2023.
[22] K. Kobayashi, Comparative Wiener–Hopf Analysis of Parallel-Plate Waveguide Cavities with Material Loading, Philos. Trans. R. Soc. A, 383, 2025.
[23] S. Simakov & S. Galyamin, Semi-infinite Cylindrical and Corrugated Waveguide Diffraction Using Wiener–Hopf–Fock Methods, arXiv:2305.04371, 2023.
[24] D. Margetis, M. Maier & M. Luskin, Wiener–Hopf Method for Surface Plasmons: Diffraction from Semi-Infinite Metamaterial Sheet, Stud. Appl. Math., 139, 599–625, 2017.
[25] D. Margetis, M. Maier & M. Luskin, Dipole Excitation of Surface Plasmons on a Conducting Sheet: FEM Approximation, J. Comput. Phys., 339, 126–145, 2017.